Mechanical Systems and Signal Processing 70-71 (2016) 995–1010

Contents lists available at ScienceDirect

Mechanical Systems and Signal Processing

journal homepage: www.elsevier.com/locate/ymssp

Multi-frequency weak signal detection based on wavelet transform and parameter compensation band-pass multi-stable stochastic resonance

Dongying Han [a,*], Pei li [b], Shujun An [b], Peiming Shi [b]

[a] College of Vehicles and Energy, Yanshan University, Qinhuangdao 066004, PR China
[b] College of Electrical Engineering, Yanshan University, Qinhuangdao 066004, PR China

ARTICLE INFO

Article history:
Received 11 October 2014
Received in revised form
21 August 2015
Accepted 1 September 2015
Available online 5 October 2015

Keywords:
Weak signal detection
Wavelet transform
Multi-stable stochastic resonance
Parameter compensation
Multi-frequency

ABSTRACT

In actual fault diagnosis, useful information is often submerged in heavy noise, and the feature information is difficult to extract. A novel weak signal detection method aimed at the problem of detecting multi-frequency signals buried under heavy background noise is proposed based on wavelet transform and parameter compensation band-pass multi-stable stochastic resonance (SR). First, the noisy signal is processed by parameter compensation, with the noise and system parameters expanded 10 times to counteract the effect of the damping term. The processed signal is decomposed into multiple signals of different scale frequencies by wavelet transform. Following this, we adjust the size of the scaled signals' amplitudes and reconstruct the signals; the weak signal frequency components are then enhanced by multi-stable stochastic resonance. The enhanced components of the signal are processed through a band-pass filter, leaving the enhanced sections of the signal. The processed signal is analyzed by FFT to achieve detection of the multi-frequency weak signals. The simulation and experimental results show that the proposed method can enhance the signal amplitude, can effectively detect multi-frequency weak signals buried under heavy noise and is valuable and usable for bearing fault signal analysis.

1. Introduction

Signal detection technology has been used in many fields, such as fault diagnosis, communications, seismic exploration and biomedical applications; therefore, it is a popular topic for researchers. The technology of signal detection can be divided into two aspects [1–3]. One is obtaining the useful signal by eliminating or suppressing the noise. Standard techniques, such as the wavelet denoising method, the adaptive filtering method, the empirical mode decomposition method, the local mean decomposition method and so on will inevitably weaken the useful signal while removing the noise. For example, the wavelet denoising method needs to select the appropriate wavelet basis; if the selection of the wavelet basis is improper, the final result will be different from the original signal. EMD has a boundary effect and produces many false mode components, which has an impact on the signal detection results [4–6].

* Corresponding author. Tel.: +86 18633503460.
E-mail address: hspace@ysu.edu.cn (D. Han).

http://dx.doi.org/10.1016/j.ymssp.2015.09.003
0888-3270/

Another detection method is stochastic resonance (SR), which can detect signals by using the noise instead of removing the noise. Stochastic resonance is a physical phenomenon, which means that a signal can be improved when the noise level is increased or when specific noise is added to the system input section. Since the concept of SR was proposed by Benzi et al. in 1981 [7], SR has been widely used in signal processing, physics, biology, large mechanical fault diagnosis and other fields [8–16]. In contrast to the traditional denoising methods, SR utilizes noise instead of eliminating it to improve the signal-to-noise ratio, allowing detection of weak signals. The output signal of a nonlinear dynamic system can be enhanced by adding noise to the system based on the SR mechanism. In recent years, SR has been a hot research topic in the field of signal processing due to its advantages in weak signal detection [17–24]. The traditional SR method focuses mainly on small-parameter signal. To achieve the detection of high frequency weak signals usually implies a need to adjust the system parameters, to scale the transformation or to use other technical means.

Many scholars have studied the detection and identification of single-frequency signals in strong noise. In practical engineering applications, however, the signal is generally multi-frequency, containing both low frequency and high frequency components. As described in the literature [25], convert the high frequency components into low frequency components by scaling, and then detect the multi-frequency signal using the bistable stochastic resonance system. Wang et al. [26] put forward a method for detecting the signal frequency by using an automatic regulation system for the frequency modulation signal and a continuous approximation of the measured signal frequency, but this method needs to know the signal frequency in advance; therefore, this method of detecting the signal has certain restrictions. Tao et al. [27] proposed a method of multi-frequency periodic weak signal detection based on a single-well potential stochastic resonance which only needs one adjustable parameter. This method can make the system reach the optimum state and is applicable in the detection of multi-frequency signals.

The majority of the existing methods for detecting multi-frequency weak signals are based on monostable or bistable stochastic resonance systems. When the signal-to-noise ratio is very low, we cannot detect the signal frequency with the bistable or monostable stochastic resonance method. The noise metastatic capacity of a multi-stable stochastic resonance system is better than the bistable stochastic resonance system; therefore, using the multi-stable stochastic resonance method to obtain frequency is more accurate than the bistable stochastic resonance method. However, there are no reports on the detection of multi-frequency weak signals using the multi-stable stochastic resonance method so far. The parameter compensation method, as opposed to double sampling, adds the signal modulation heterodyne method and does not need to know the frequency of the signal and is not affected by sampling frequency. In addition, it only needs to know the approximate frequency of the signals, which makes it easier to detect the high frequency signals.

In this paper, a novel weak signal detection method based on wavelet transform and parameter compensation to produce a band-pass multi-stable stochastic resonance is proposed. The rest of this paper is organized as follows. Section 2 provides a brief introduction to the principles of multi-stable SR and describes how to construct a common model for multi-stable SR. Section 3 introduces the decomposition of multi-scale wavelets. Section 4 describes the method of parameter compensation and compares the performance of the proposed method with the simulation and experimental data, as well as presenting the computational results for an experimental example. Finally, Section 5 provides the conclusions.

2. Principles of multi-stable SR

The model for multi-stable SR is a multi-stable nonlinear system driven by periodic signals and white noise. It takes advantage of the synergistic effects between the input signal and noise in the nonlinear system, transferring noise energy into useful signals that resonate, thus achieving the identification weak signals. The Langevin equation can be written as follows [28]:

$$dx/dt = k[\,-dU(x)/dx + s(t) + \eta(t)] \tag{1}$$

where k is the relaxation time scale, $s(t) = \sum_{i=1}^{n} A_i \sin(2\pi f_i t)$ is the input signal, A_i is the periodic signal amplitude, f_i is the driving frequency, and $\eta(t) = \sqrt{2D}\,\varepsilon(t)$ with $<\eta(t)\eta(t+\tau)> = 2D\delta(t)$ representing the noise item, in which D is the noise intensity and $\varepsilon(t)$ represents Gaussian white noise with zero mean and unit variance.

The multi-stable nonlinear system $U(x)$ driven by the periodic signal and white noise generates the output stochastic resonance response $x(t)$, as shown in Fig. 1.

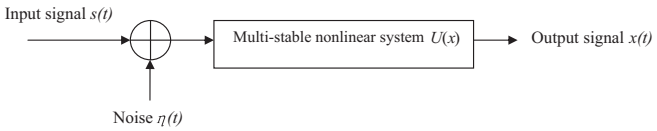

Fig. 1. Multi-stable nonlinear system.

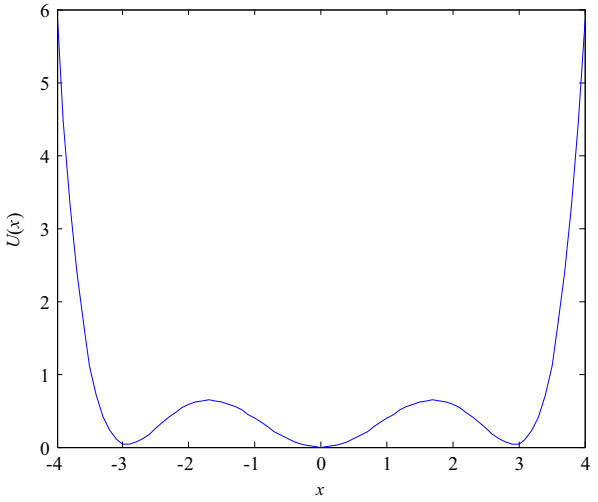

Fig. 2. The multi-stable potential function $U(x)$.

For the multi-stable potential model, $U(x)$ represents a potential function:

$$U(x) = \frac{x^6}{6a'} - \frac{(1+c)x^4}{4b'} + \frac{c}{2}x^2 \tag{2}$$

where a', b' and c denote the barrier parameters of the multi-stable potential with positive real values and $b'=5$, $c>0$, $a'=20+5c$ $(0<c<1)$, $a=27.5-2.5c(1<c<3)$.

The above equation has three stable solutions and two unstable solutions as shown in Fig. 2.

Eq. (1) can be rewritten as:

$$\frac{dx}{dt} = k\left[-\frac{x^5}{a'} + \frac{(1+c)x^3}{b'} - cx + \sum_{i=1}^{n} A_i \sin(2\pi f_i t) + \eta(t)\right] \tag{3}$$

When $\sum_{i=1}^{n} A_i \sin(2\pi f_i t) + \eta(t)=0$, the potential energy is minimum and the system is most stable at the lowest point. When a weak periodic signal is input to the system, the signal energy cannot overcome the blocking of the barrier and the output state only moves within a potential well. If noise is input into the system, the noise energy will be partially transferred to the signal to produce interactions, overcoming the system barrier. Thus the system transitions among the three steady states. Because the potential difference between two of the three steady states is much larger than the amplitude of the input signal, the output signal amplitude is greater than the input signal amplitude, which illustrates the SR phenomenon.

3. Decomposition of a multi-scale wavelet

3.1. Discrete wavelet transform

The wavelet transform can extract the weak signal components from the original signal using multi-resolution decomposition and has very good localization ability [29].

Take a basic function $\varphi(t)$:

$$\varphi_{a,b}(t) = \frac{1}{\sqrt{a}}\varphi\left(\frac{t-b}{a}\right) \tag{4}$$

where a is the dilation factor and b is the frequency shift factor. $\varphi_{a,b}(t)$ is obtained by the dilation and translation of $\varphi(t)$. By changing $a$and b, a family of functions can be obtained. Suppose $x(t) \in L^2(R)$, then use wavelet bases $\varphi(t)$ to transform $x(t)$ using the discrete wavelet bases. The wavelet transform coefficient is

$$WT_x(a, b) = \frac{1}{\sqrt{a}} \int x(t)\varphi^*\left(\frac{t-b}{a}\right)dt \tag{5}$$

where a, b and t are continuous variables. Therefore, Eq. (4) is the continuous wavelet transform.

The discrete wavelet is obtained by providing discrete parameters for the continuous wavelet function [30]. First, taking $a = a_1^j,\ a_1 > 0,\ j \in Z$, then the corresponding wavelet function is $a_1^{-j/2}\varphi(a_1^{-j}t - a_1^{-j}b),\ j \in Z$. After letting $b = a_1^j k b_1$, the interval on the time axis is $a_1^j b_1$. Usually the discrete mode of the wavelet is binary discrete; when $a_1=2$ we can get $a = 2^j$, $b = 2^j k b_1$, then the corresponding wavelet function is $2^{-j/2}\varphi(2^{-j/2}t - kb_1)\ j \in Z$. Further normalizing b_1, we get

$$\varphi_{j,k}(t) = 2^{-j/2}\varphi(2^{-j}t - k),\ \ j \in Z \tag{6}$$

Then, each transform coefficient is

$$W_{Tx}(2^j, 2^j k) = \frac{1}{\sqrt{2^j}}\sum_n \varphi^*\left(\frac{n}{2^j} - k\right)x(n) \tag{7}$$

3.2. Wavelet decomposition and reconstruction

This paper chose the Daubechies wavelet, which can use *dbN* for decomposition and reconstruction [31]. For arbitrary $f(t) \in L^2(R)$, this can be expressed as

$$f(t) = \sum_j f_j(t) + \sum_j g_j(t) = \sum_j \sum_k c_{j,k}\varphi_{j,k}(t) + \sum_j \sum_k d_{j,k}\psi_{j,k}(t) \tag{8}$$

where $f_j(t)$, called the smooth partial or approximate part, is the low frequency part of $f(t)$, and $g_j(t)$, called the details part, is the high frequency part of $f(t)$. $\varphi(t)$ is the base function of the Daubechies wavelet decomposition and $\varphi_{j,k}(t)$ is obtained by the dilation and translation of $\varphi(t)$. $\psi(t)$ is a scaling function; $\psi_{j,k}(t)$ is obtained by the dilation and translation of $\psi(t)$. $c_{j,k}$ are the coefficients of the approximate wavelet, $d_{j,k}$ are the coefficients of the details wavelet. They are expressed as:

$$\varphi_{j,k}(t) = 2^{-j/2}\varphi(2^{-j}t - k) \tag{9}$$

$$\psi_{j,k}(t) = 2^{-j/2}\psi(2^{-j}t - k) \tag{10}$$

$$c_{j,k} = \left\langle f(t), \varphi_{j,k}(t)\right\rangle = \int_R f(t)\overline{\varphi_{j,k}(t)dt} \tag{11}$$

$$d_{j,k} = \left\langle f(t), \psi_{j,k}(t)\right\rangle = \int_R f(t)\overline{\psi_{j,k}(t)dt} \tag{12}$$

Regulate the size of the different scaled signals' amplitudes, and reconstruct the signal; then the signal can be expressed as:

$$f(t) = \sum_j \sum_k K_i {c_{j,k}}^m \varphi_{j,k}(t) + \sum_j \sum_k K_i {d_{j,k}}^n \psi_{j,k}(t) \tag{13}$$

where K_i is a scale contraction factor, which can adjust the size of the amplitude; in addition, both m and n are positive integers.

Decompose the noised-signal, the noise is usually included in the high frequency part of the decomposition series, so we can use the threshold to process the wavelet coefficient. In this paper, in the process of simulation, constantly adjust the threshold, select the optimal value to get the best simulation effect.

Scale contraction factor K_i is also can adjust, We usually turn the low frequency signal wavelet coefficient a little higher, while turn the high frequency part of the decomposition coefficient a little lower.

4. Multi-frequency signal detection method based on parameter compensation for multi-stable stochastic resonance

4.1. Principles of parameter compensation

The traditional SR method mainly focuses on small parameters, including very low driving frequency, low amplitude and low noise intensity. Those signals which have very high driving frequency or strong noise intensity often need indirect methods to implement stochastic resonance, such as double sampling, heterodyning, modulation and parameter compensation, etc. Except for parameter compensation, the other methods all need to know the signal frequency and have to choose the appropriate sampling frequency, which is difficult to determine for high frequency signals [32–34]. To address high frequency signals, this paper chose the parameter compensation method, which does not need to know the frequency of the signal and is not affected by sampling frequency and, finally, achieves the purpose of detecting the weak signal.

The principles of the parameter compensation method are shown as follows:

Suppose the input signal $s(t) = \sum_{i=1}^{n} A_i \sin(2\pi f_i t)$, and we integrate on both sides of Eq. (3), we obtain the following equation:

$$\begin{aligned} x(t) &= k\left\{ \int\left[-\frac{x^5}{a} + \frac{(1+c)x^3}{b} - cx + \sum_{i=1}^{n} A_i \sin(2\pi f_i t) + \eta(t) \right]dt \right\} \\ &= k\left\{ \int\left[-\frac{x^5}{a} + \frac{(1+c)x^3}{b} - cx \right]dt + \int\left[\sum_{i=1}^{n} A_i \sin(2\pi f_i t) \right]dt + \int [\eta(t)]dt \right\} \\ &= k\left\{ \int\left[-\frac{x^5}{a} + \frac{(1+c)x^3}{b} - cx \right]dt - \sum_{i=1}^{n} \frac{A_i}{2\pi f_i} \cos(2\pi f_i t) + \int [\eta(t)]dt \right\} \end{aligned} \tag{14}$$

From Eq. (14), we can see that the amplitude of the input signal $s(t)$ has been reduced by the original signal $1/2\pi f_i$ after passing through the multi-stable stochastic resonance system, and the amplitudes increase with increasing frequency, therefore, we cannot detect the presence of the high frequency signals in the output signal even though the high frequency signal has been processed by the multi-stable SR system. To solve this problem, we use the parameter compensation method that joins an amplification link in the Langevin equation, that is to say, dividing Eq. (8) by a constant on the right side, which can offset the trend of the amplitude getting smaller.

Theoretically, k is equal to $\max\{2\pi f_i\}$, but in the actual simulation analysis, to ensure the required effect, the value of k is slightly larger than $\max\{2\pi f_i\}$.

Frequency range (Hz)	0–1	1–100	100–1000	1000–5000
Compensation parameters (k)	$\geq 2\pi$	$\geq 200\pi$	$\geq 2000\pi$	$\geq 10{,}000\pi$

In practical applications the vibration signal usually has multiple frequencies and is submerged in such strong background noise that it is difficult to achieve the identification and extraction of the signal. In this paper, a novel method is proposed that uses multi-frequency weak signal detection methods based on wavelet transform and parameter compensation band-pass multi-stable stochastic resonance. The schematic diagram is shown in Fig. 3.

First the noisy signal is processed by parameter compensation. It is then decomposed into a number of scaled components using DWT. We resynthesize them by adjusting the factor of each scale, so that the target frequency can be enhanced by the SR system. Finally they are processed through a band-pass filter, leaving only the enhanced sections of the signal, thus achieving multi-frequency detection of weak signals.

4.2. Simulation experimental verification

Three sine signals are selected as the simulated signals. The test signals are generated according to the equation below:

$$s(t) = 0.1\sin(2\pi \times 10 \times t) + 0.3\sin(2\pi \times 80 \times t) + 0.2\sin(2\pi \times 600 \times t) + \eta(t),$$

where $\eta(t)$ is the noise intensity. The simulated signals and their frequency spectrum are shown in Fig. 4. As seen, there are obvious periodic shocks in the time-domain waveform and the energy distribution of the spectrum has a wide range. The signal frequency is extremely weak; therefore, that it is hard to find obvious vibration characteristics at low frequencies.

Fig. 5 shows the time domain and frequency domain plots after passing through the multi-stable SR system. It can be seen that there are two obvious spikes, but their amplitudes are still weak; therefore, they are difficult to detect in the output signal. In addition, there are three frequencies in the input signal, but we can only detect two obvious frequencies in the output, which shows that sometimes we cannot accurately detect multi-frequency weak signals using multi-stable stochastic resonance alone.

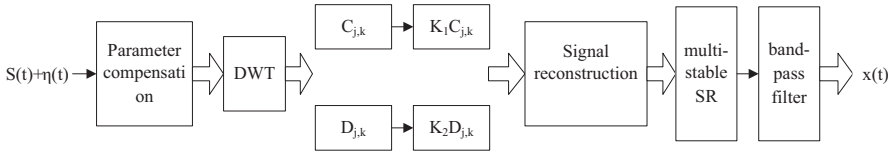

Fig. 3. The principle diagram of multi-frequency weak signal detection based on wavelet transform and parameter compensation band-pass multi-stable stochastic resonance.

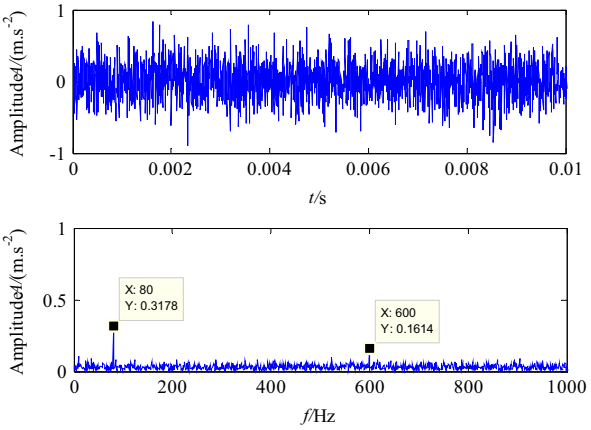

Fig. 4. The time-domain waveform and frequency spectrum of the simulated signal.

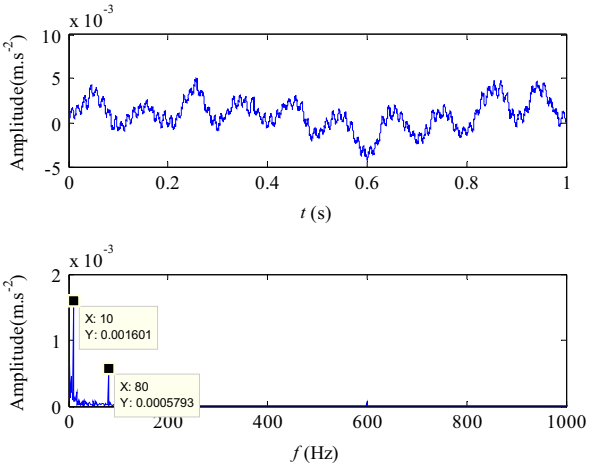

Fig. 5. The time-domain waveform and frequency spectrum of the output signal.

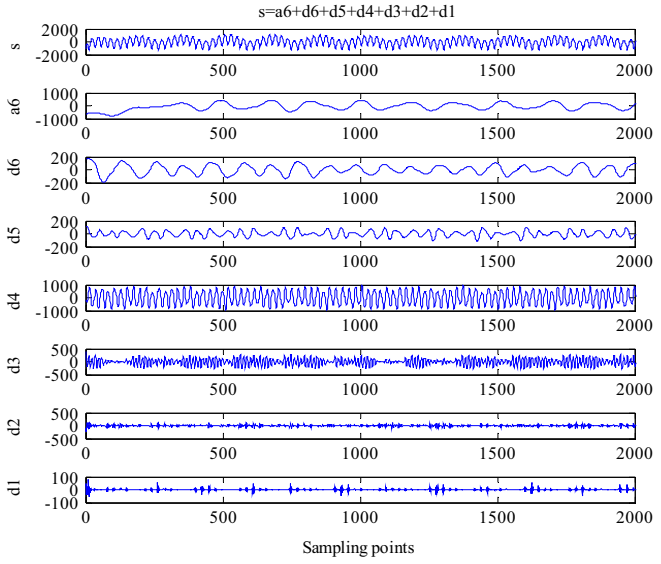

Fig. 6. The processed signal's decomposition result after DWT.

Now we use the method proposed in this paper to detect weak signals. First, process the signal using parameter compensation and let $k = 4000$; we then obtain the following equation:

$$\frac{dx}{dt} = 4000 \times \left[-\frac{dU(x)}{dx} + 0.1\sin(2\pi \times 10 \times t) + 0.3\sin(2\pi \times 80 \times t) + 0.2\sin(2\pi \times 600 \times t) + \eta(t) \right] \tag{16}$$

Fig. 6 shows the processed signal's decomposition result after DWT. The decomposition scale is set to $J=6$. In the multi-scale wavelet decomposition, take traversing method to select the decomposition scale. That is to set the decomposition scale as $J=3$, 4, 5, 6, 7, 8, and then find out the value of J to get the best decompose effect.

As seen from Fig. 6, s is the processed signal, a6 is the low frequency part of the signal, and d1–d6 are the high frequency parts of the signal. Further adjust the size of the scaled signals' amplitudes and reconstruct the signals; the output signals after passing through the multi-stable SR system are shown in Fig. 7. It can be seen that some of the high-frequency components are weakened and the targeted frequencies are enhanced. The amplitude of the 10 Hz frequency (the simulated signal frequency within the error range) changes from 0.1 to 1.015. The amplitude of the 80 Hz frequency changes from 0.3 to 2.619. The amplitude of the 600 Hz frequency changes from 0.2 to 0.4426.

The different frequency bands signal are filtered. Each resonance band is retained after band-pass filter processing only. Fig. 8 shows the time domain and frequency domain plots after the band-pass filter. Finally, the signal is synthesized to obtain the ideal frequency enhancement effect, as shown in Fig. 9, which effectively shows that the simulated signal frequencies exist. Therefore, this study verified the effectiveness of the method.

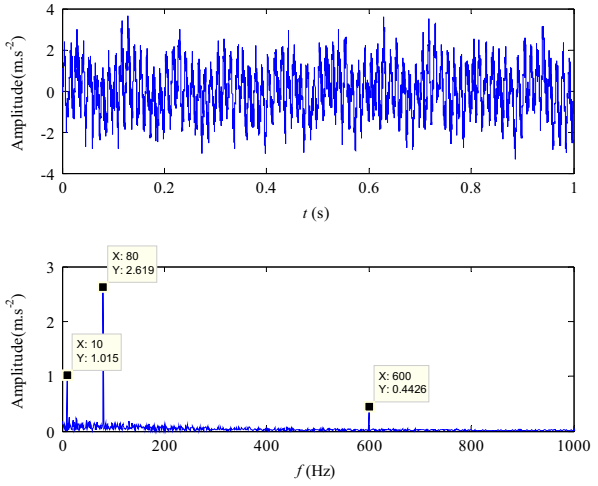

Fig. 7. The time-domain waveform and frequency spectrum of the output signals after the multi-stable SR system.

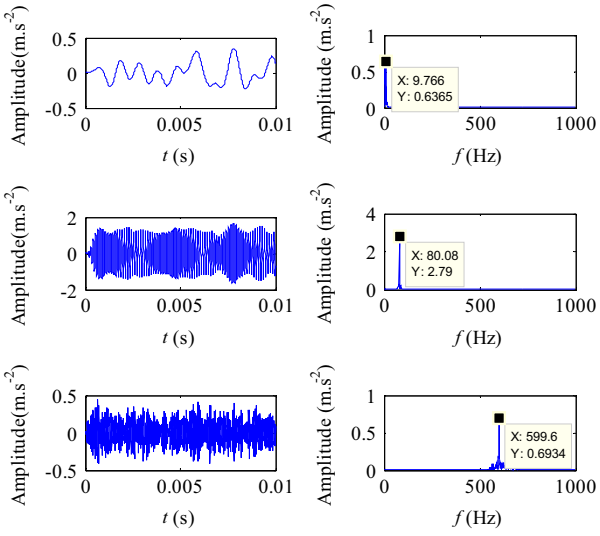

Fig. 8. The time-domain waveform and frequency spectrum of the output signal after the band-pass filter.

To illustrate the advantages of the variable scale multi-stable stochastic resonance method, we compare it with the bistable stochastic resonance method. Using the signal in Fig. 9, after a series of analyses of the output signal time-frequency diagram, the result is as shown in Fig. 10.

Comparing Fig. 9 to Fig. 10, it can be seen that both methods can detect the signal frequency, but the peak amplitude on the peak amplitude diagram in Fig. 9 is much higher than is visible in the bistable system. The multi-stable system can transfer more energy to the useful signal, and the signal energy enhancement amplitude increases, that is, the performance

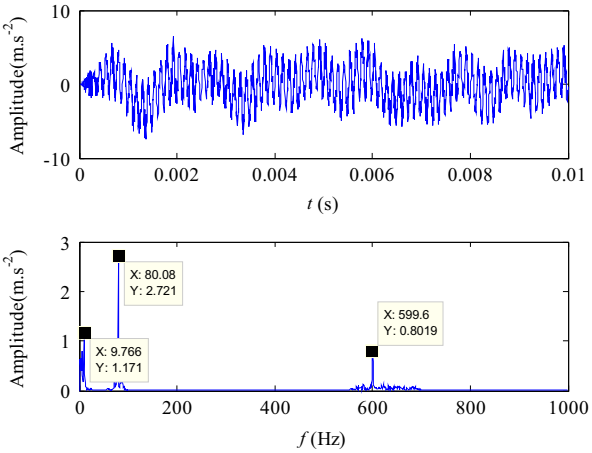

Fig. 9. The time-domain waveform and frequency spectrum of the synthesized signal for different bands.

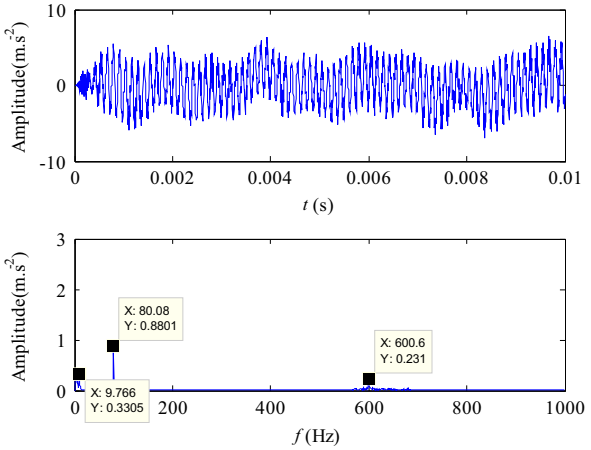

Fig. 10. Time frequency map for the bistable output signal.

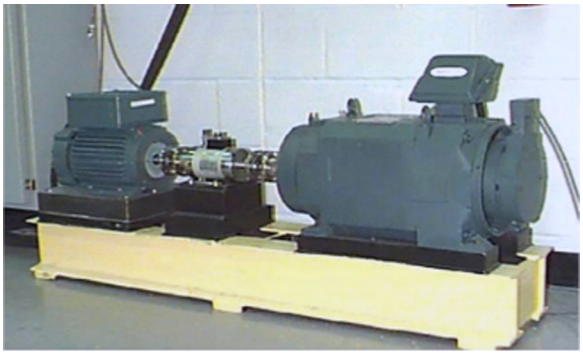

Fig. 11. The bearing test stand from CWRU.

of the multi-stable stochastic resonance method is better than the performance of the bistable stochastic resonance method, with a more significant effect on the detection of the weak signals.

4.3. Analysis of rolling bearing faults

To verify the effectiveness and efficiency of the proposed method in practical applications, we analyzed sets of data from bearings carrying fault information using the method shown in Fig. 3.

Rolling bearing fault signals are typically non-stationary, modulated and weak, making it hard to detect and extract feature information, which is often submerged in strong background noise. In this paper, the data are from the Case Western Reserve University (CWRU) Bearing Data Center website [35]. The data were originally acquired using the experimental setup shown in Fig. 11. The bearings used in this test are deep groove ball bearings of the type 6205-2RS JEM SKF, the motor speed is f_r=1750 rpm (29.17 Hz), and the sampling frequency is 12 kHz. The details of the geometry of this type of bearing are provided in Table 1 and the characteristic frequencies are shown in Table 2. Taking the inner raceway faults as an example, calculating the feature frequency leads to 157.961 Hz; twice this is 315.922 Hz, and triple is 473.883 Hz.

The inner raceway fault signal and its spectrum diagram are shown in Fig. 12, where can be seen that there are obvious periodic shocks in the time-domain waveform and that the fault characteristic frequency can hardly be seen in the waveform due to the heavy background noise interference. Then, we use the method proposed in this paper to detect weak signals. First, process the signal by parameter compensation.

Fig. 13 shows the processed signal's decomposition result after DWT. The decomposition scale is set to J=6. Further adjust the size of the scaled signal's amplitude and reconstruct the signals; the output signals after passing through the multi-stable SR system are show in Fig. 14. It can be seen that some of the high-frequency components are weakened and the targeted frequencies are enhanced.

The different frequency bands signal are filtered. Each resonance band is retained after band-pass filtering process only. Fig. 15 shows the time domain and frequency domain plots after band-pass filter processing only. Finally, the signal is synthesized to obtain the ideal frequency enhancement effect, as shown in Fig. 16. It can be seen that the amplitude of the 157.5 Hz frequency (the feature frequency within the error range) changes from 0.04945 to 4.487. The amplitude of the

Table 1
The main parameters of the rolling bearings.

Inner diameter (mm)	Outer diameter (mm)	Pitch diameter (mm)	Ball diameter (mm)	Ball number	Contact angle/(°)
25.001	51.999	39.040	7.940	10.000	0

Table 2
Rolling bearing fault feature frequency.

Bearing element	Inner ring	Outer ring	The retainer	Rolling body
Failure frequency	5.4152 f_r	3.5848 f_r	0.39828 f_r	4.7135 f_r

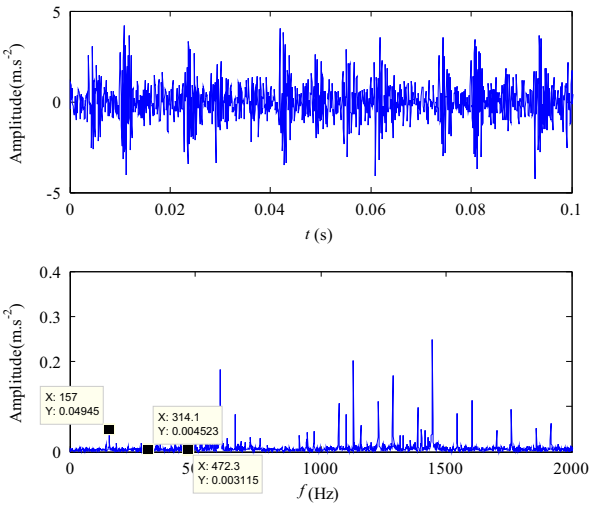

Fig. 12. The time-domain waveform and frequency spectrum of inner raceway fault signal.

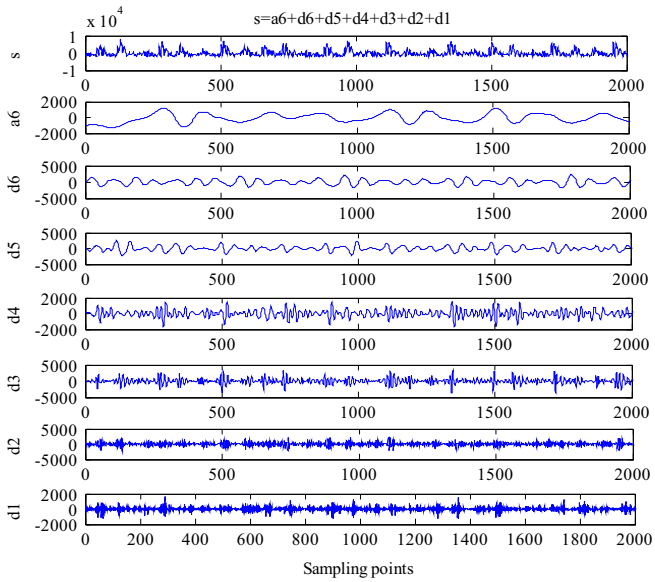

Fig. 13. The processed signal's decomposition result after DWT.

314.9 Hz feature changes from 0.004543 to 2.067. The amplitude of the 472.4 Hz feature changes from 0.003115 to 0.6882. This effectively shows that the rolling bearing race fault exists.

To illustrate again the advantages of the variable scale multi-stable stochastic resonance method, we compare it to the bistable stochastic resonance method. Using the signal in Fig. 16, after a series of analyses of the output signal time-frequency diagram, the result is as shown in Fig. 17.

Comparing Figs. 16 and 17 we can see that the multi-stable stochastic resonance and the bistable stochastic resonance can detect the weak signal, but in the former the fault frequency amplitude is greater than in the latter, i.e., the noise energy transfer capability is stronger.

4.4. Analysis of gear faults

We analyzed sets of data from gear fault information using the method shown in Fig. 3. The data are from Qian Peng diagnosis engineering co., LTD. The number of the driving gear's teeth is 55, the number of the driven gear's teeth is 75, and we cut off a driven gear's teeth, as shown in Fig. 18.

The broken tooth gear's spectrum displays as a meshing frequency on the center and on both sides of the meshing frequency have the uniform distribution of the harmonic frequency. But the interval of the harmonic frequency is the broken gear's rotating frequency.

The meshing frequency of the gear is

$$f_m = \frac{n}{60} z_1 = \frac{878}{60} \times 55 = 804.8 \text{ Hz } f_m = \frac{n}{60} z_1 = \frac{878}{60} \times 55 = 804.8 \text{ Hz}$$

The rotating frequency of the driven gear is

$$f_r = \frac{n_2}{60} = \frac{n}{60} \times \frac{z_1}{z_2} = \frac{878}{60} \times \frac{55}{75} = 10.7 \text{ Hz}$$

where n is the engine's rotating speed, n_2 is the driven gear's rotating speed, z_1 is the number of the driving gear, z_2 is the number of the driven gear.

The gear fault signal and its spectrum diagram are shown in Fig. 19, where can be seen that there are obvious periodic shocks in the time-domain waveform, but the fault characteristic frequency can hardly be seen in the frequency spectrum map due to the heavy background noise interference. So we must process the gear fault signal with other effective means. The time-domain waveform and frequency spectrum map of output signals after passing through the bistable SR system are show in Fig. 20. The time-domain waveform and frequency spectrum map of output signals after passing through the multi-stable SR system are show in Fig. 21.

Figs. 20 and 21 show that the frequency 804.8 Hz of the broken gear tooth fault feature frequency is the center the frequency spectrum, and on both sides of this frequency respectively distribute 772.7 Hz, 783.6 Hz, 794.6 Hz, 815.7 Hz,

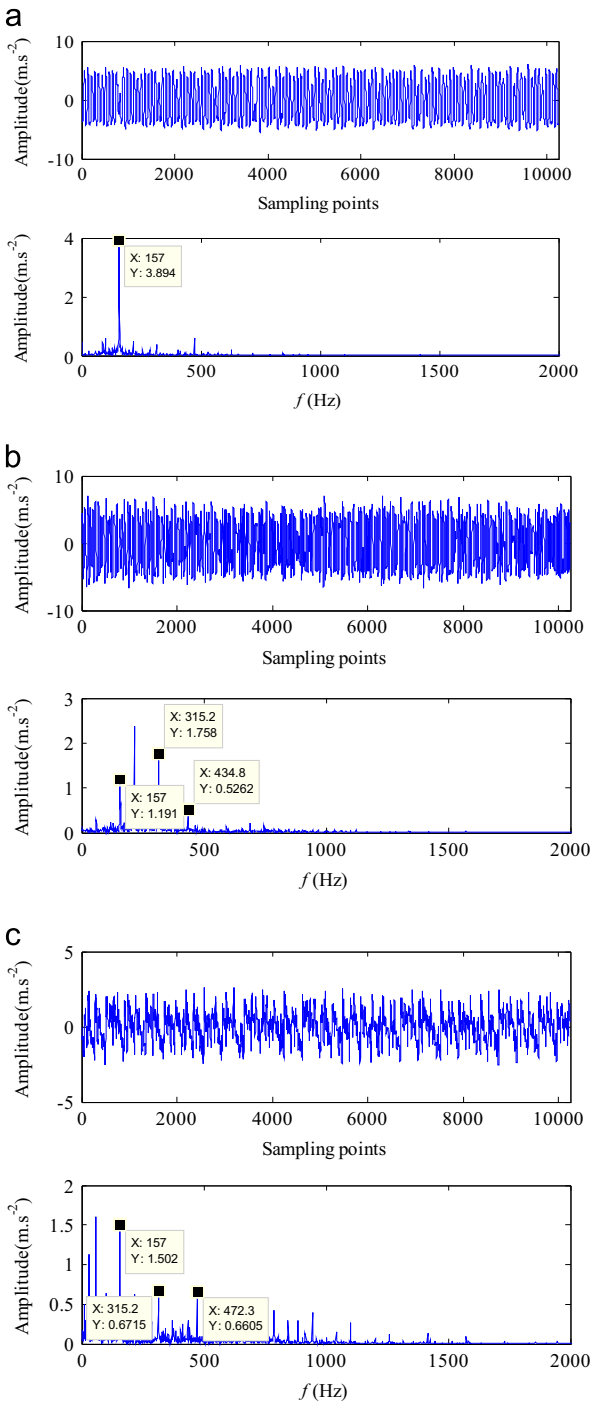

Fig. 14. The time-domain waveform and frequency spectrum of the output signals after multi-stable SR system.

825.9 Hz and 836.8 Hz etc. several obvious frequency. The 804.8 Hz is the gear meshing frequency. The 772.7 Hz, 783.6 Hz, 794.6 Hz, 815.7 Hz, 825.9 Hz and 836.8 Hz are the harmonic frequency. The broken tooth gear's rotating frequency is the same with the sideband's frequency interval; it clearly shows the frequency characteristics of the broken tooth gear.

Comparing Figs. 20 and 21 we can see that the multi-stable stochastic resonance and the bistable stochastic resonance both can detect the weak signal, but in the former the fault frequency amplitude is greater than in the latter. It shows that the multi-stable stochastic resonance is stronger than the bistable stochastic resonance on enhanced weak signal capability.

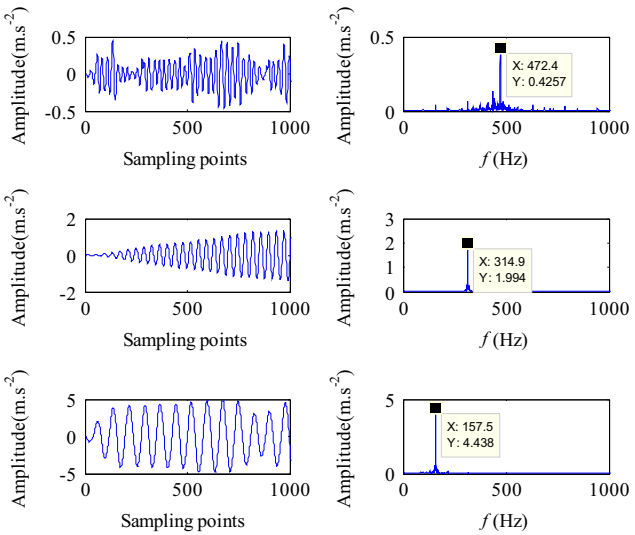

Fig. 15. The time-domain waveform and frequency spectrum of the output signal after the band-pass filter.

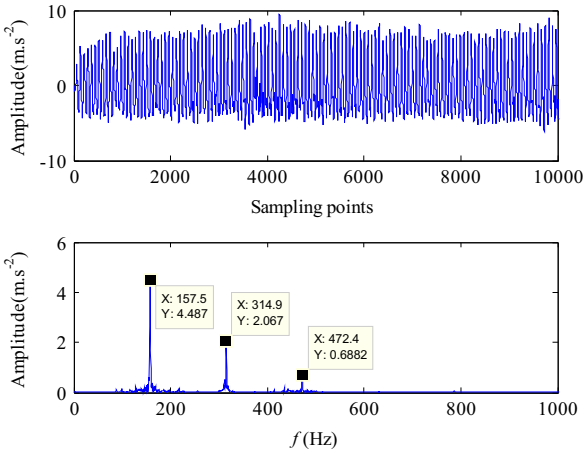

Fig. 16. The time-domain waveform and frequency spectrum of synthesized signal for different bands.

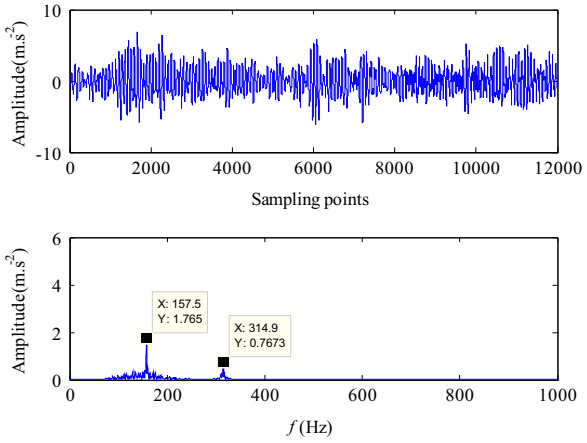

Fig. 17. Time frequency map bistable output signal.

The amplitude comparison chart of original signal, bistable stochastic resonance system output signal and multi-stable stochastic resonance system output signal is shown in Fig. 22. Fig. 23 shows the local amplification in Fig. 22. We clearly see that the fault frequency amplitude of the multi-stable stochastic resonance system is lagerer by than the bistable stochastic

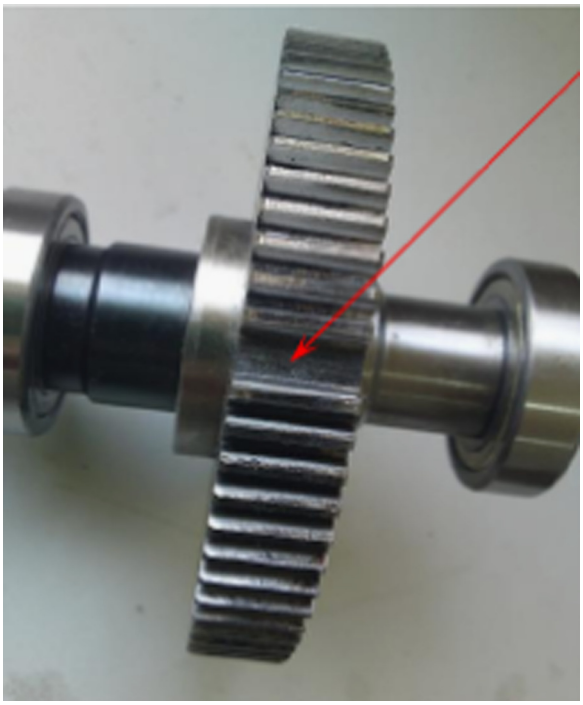

Fig. 18. The fault Gear with Broken Teeth.

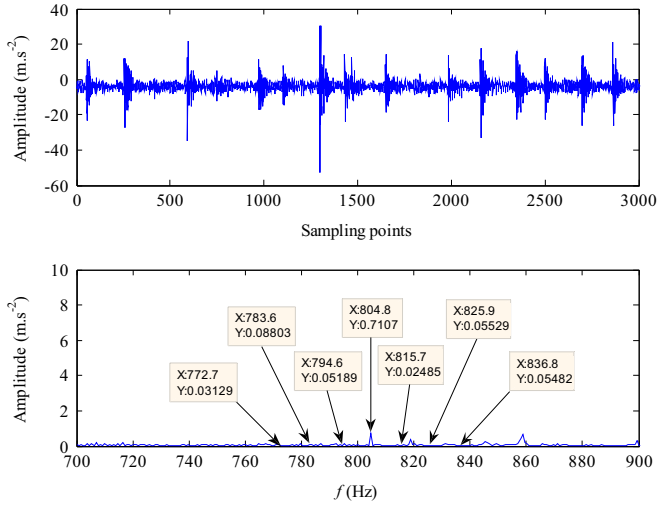

Fig. 19. The time-domain waveform and frequency spectrum map of gear fault signal.

resonance system. The amplitude the multi stable stochastic resonance system is greater than the bistable stochastic resonance system output signal.

5. Conclusions

A novel weak signal detection method based on wavelet transform and parameter compensation band-pass multi-stable stochastic resonance is proposed. We reach the following conclusions:

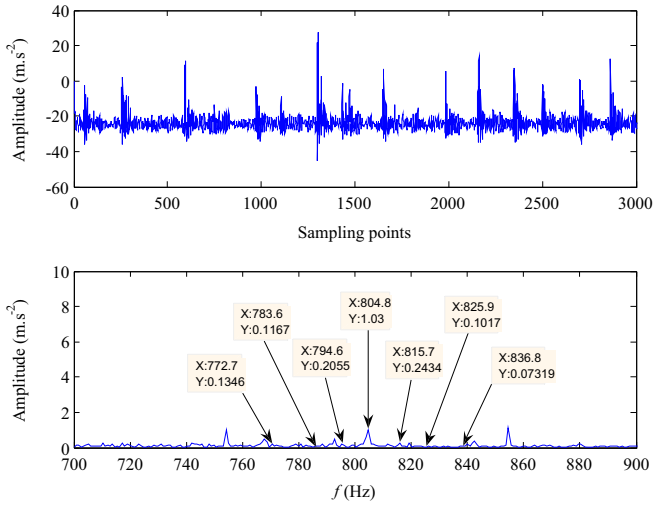

Fig. 20. The time-domain waveform and frequency spectrum map of bistable SR system output signal.

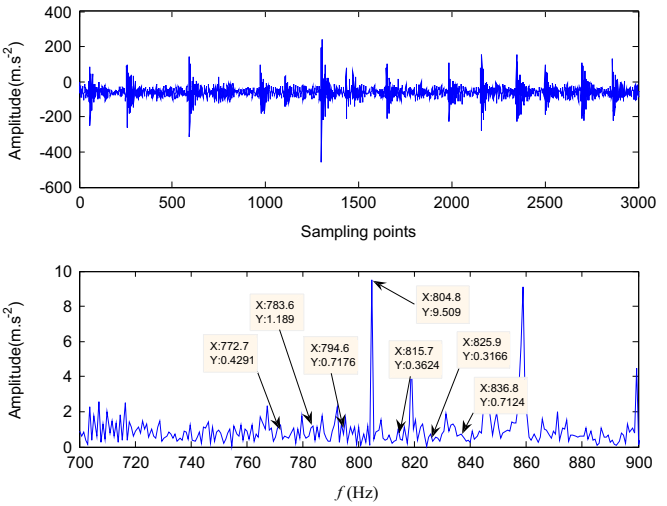

Fig. 21. The time-domain waveform and frequency spectrum map of multi-stable SR system output signal.

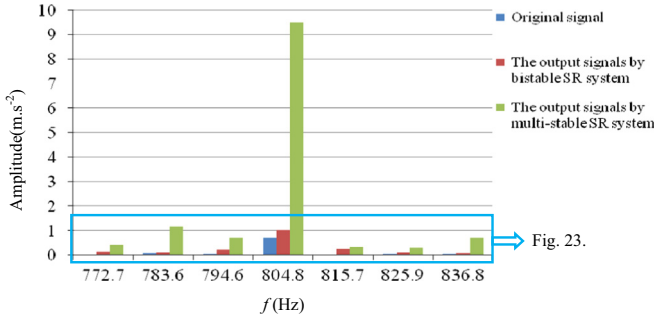

Fig. 22. Amplitude comparison chart.

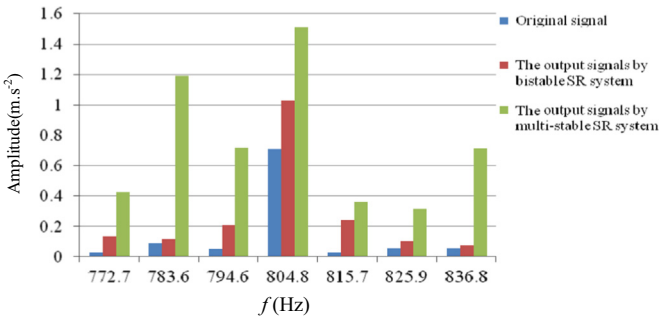

Fig. 23. Local amplification in Fig. 22.

(1) It is beneficial to improve the output energy system by adjusting the amplitude of the wavelet multi-scale decomposition signal.
(2) The parameter compensation method, which is widely used, makes the high frequency signal detection process simple. The combined parameter compensation method combined with the stochastic resonance method can lead to the detection of multiple high-frequency weak signals.
(3) The metastatic ability of noise is stronger using the multi-stable stochastic resonance method than using the bistable stochastic resonance method; the proposed method also can greatly enhance the signal amplitude.
(4) Through the analysis of simulation experiments and a real-world examples, the results show that this method can effectively detect multi-frequency weak signals submerged in noise. The test results are clear and accurate.

Acknowledgments

This work was supported by the National Natural Science Foundation of China (51475407 and 51104129) and Hebei Provincial Natural Science Foundation of China (No. E2015203190) and Key Project of Natural Science Research in Colleges and Universities of Hebei Province (No. ZD2015050). The authors would like to thank CWRU for providing the free bearing data download, and the anonymous reviewers for their valuable comments and suggestions.

References

[1] P. Shi, X. Ding, D. Han, Study on multi-frequency weak signal detection method based on stochastic resonance tuning by multi-scale noise, . 47 (2014) 540–546 Measurement 47 (2014) 540–546.
[2] M. Gong, F. Guo, Phenomenon of stochastic resonance in a time-delayed bistable system driven by colored noise and square-wave signal, Chin. J. Phys. 49 (2011) 655–663.
[3] P. Goldman, A. Muszynska, Application of Full Spectrum to Rotating Machinery Diagnostics, Orbit, 17–21, Bently Nevada Corporation, USA, 1st Quarter, 1999.
[4] W. Sun, J. Chen, J. Li, Decision tree and PCA-based fault diagnosis of rotating machinery, Mech. Syst. Signal Process. 21 (2007) 1300–1317.
[5] F. Wu, T. Wang, J. Lee, An online adaptive condition-based maintenance method for mechanical system, Mech. Syst. Signal Process. 24 (2010) 2985–2995.
[6] T. Galka, M. Tabaszewski, An application of statistical symptoms in machine condition diagnostics, Mech. Syst. Signal Process. 25 (2011) 253–265.
[7] R. Benzi, A. Sutera, A. Vulpiani., The mechanism of stochastic resonance, J. Phys. A 14 (1981) L453.
[8] B. Kosko, S. Mitaim, Robust stochastic resonance: signal detection and adaptation in impulsive noise, Phys. Rev. E 64 (2001) 051110.
[9] S. Zozor, P.O. Amblard, Stochastic resonance in discrete-time nonlinear AR(1) models, IEEE Trans. Signal Process. 47 (1) (1999) 108–122.
[10] S. Zozor, P.O. Amblard, Erratum: stochastic resonance in discrete time nonlinear AR(1) models, IEEE Trans. Signal Process. 49 (5) (2001) 1107–1109.
[11] S. Zozor, P.O. Amblard, On the use of stochastic resonance in sine detection, Signal Process. 7 (2002) 353–367.
[12] F.B. Duan, F. Chapeau-Blondeau, D. Abbott, Fisher-information condition for enhanced signal detection via stochastic resonance, Phys. Rev. E 84 (2011). (051107_1–051107_5).
[13] V.N. Hari, G.V. Anand, A.B. Premkumar, A.S. Madhukumar, Design and perfor-mance analysis of asignal detector based on suprathreshold stochastic resonance, Signal Process. 92 (2012) 1745–1757.
[14] F.B. Duan, D. Abbott, Signal detection for frequency-shift keying via short-time stochastic resonance, Phys. Lett. A 344 (2005) 401–410.
[15] F.B. Duan, D. Abbott, Binary modulated signal detection in a bistable receiver with stochastic resonance, Physica A 376 (2007) 173–190.
[16] F. Chapeau-Blondeaua, F.B. Duan, D. Abbottc, Signal-to-noise ratio of a dynamical saturating system: switching from stochastic resonator to signal processor, Physica A 387 (2008) 2394–2402.
[17] F.B. Duan, F. Chapeau-Blondeau, D. Abbott, Exploring weak-periodic-signal stochastic resonance in locally optimal processors with a Fisher information metric, Signal Process. 92 (2012) 3049–3055.
[18] D. Rousseau, F. Chapeau–Blondeau, Suprathreshold stochastic resonance and signal-to-noise ratio improvement in arrays of comparators, Phys. Lett. A 321 (2004) 280–290.
[19] D. Rousseau, F. Chapeau–Blondeau, Stochastic resonance and improvement by noise in optimal detection strategies, Digit. Signal Process. 15 (1) (2005) 19–32.
[20] D. Rousseau, G.V. Anandb, F. Chapeau–Blondeau, Noise-enhanced nonlinear detector to improve signal detection in non-Gaussian noise, Signal Process. 86 (2006) 3456–3465.
[21] Q. He, J. Wang, Y. Liu, D. Dai, F. Kong, Multiscale noise tuning of stochastic resonance for enhanced fault diagnosis in rotating machines, Mech. Syst. Signal Process. 28 (2012) 443–457.
[22] D. Han, X. Ding, P. Shi, Multi-frequency weak signal detection based on EMD after de-noising by. adaptive re-scaling frequency-shifted band-pass stochastic resonance, J. Mech. Eng. 49 (2013) 10–18.
[23] J. Liang, S. Yang, Z. Tang, Weak signal detection based on stochastic resonance, J. Electron. Inf. Technol 28 (2006) 1068–1072.
[24] M. Zvokelj, S. Zupan, I. Prebil, Non-linear multivariate and multiscale monitoring and signal denoising strategy using Kernel principle component analysis combined with ensemble empirical mode decomposition method, Mech. Syst. Signal Process. 25 (2011) 2631–2653.

[25] Q. He, J. Wang, Effects of multiscale noise tuning on stochastic resonance for weak signal detection, Digit. Signal Process. 22 (2012) 614–621.
[26] Z. Wang, J. Chen, G. Dong, Yu Zhou, Constrained independent component analysis and its application to machine fault diagnosis, Mech. Syst. Signal Process. 25 (2011) 2501–2512.
[27] Z. Tao, C. Lu, Z. Cha, et al., Multi-frequence periodic weak signal detection based on single-well potential stochastic resonance, J. Eectron. Meas. Instrum. 28 (2014) 171–176.
[28] Q. Mao, M. Lin, Y. Zheng, Study of weak multi-frequency signal detection based on stochastic resonance, J. Basic Sci. Eng. 16 (2008) 86–91.
[29] H. Riske, The Fokker–Planck Equation-Methods of Solution and Applications, Springer, Berlin, 1989, 1–20.
[30] J. Raja, B. Muralikris, S. Fu, Recent advances in separat ion of roughness, waviness and form, Precis. Eng. 26 (2002) 22–235.
[31] W. Zhao, J. Liu, Y. Yin, Medium-low frequency signal detection based on stochastic resonance principle, Chin. J. Sci. Instrum. 32 (2011) 721–728.
[32] N. Li, R. Zhou, Q. Hu, X. Liu, Mechanical fault diagnosis based on redundant second generation wavelet packet transform, neighborhood rough set and support vector machine, Mech. Syst. Signal Process. 28 (2012) 608–621.
[33] Y. Lei, D. Han, J. Lin, et al., New adaptive stochastic resonance method and its application to fault diagnosis, J. Mech. Eng. 48 (2012) 62–67.
[34] G. Zhu, K. Ding, Y. Zhang, et al., Experimental research of weak signal detection based on the stochastic resonance of nonlinear system, Acta Phys. Sin. 59 (2010) 3001–3006.
[35] http://www.csegroups.case.edu/bearingdatacenter/pages/12k-driveend-bearing-fault-data).